

PRPS2 mutations drive acute lymphoblastic leukemia relapse through influencing PRPS1/2 hexamer stability

Lili Song^a, Peifeng Li^b, Huiying Sun^a, Lixia Ding^a, Jing Wang^b, Benshang Li^a, Bin-Bing S. Zhou^a, Haizhong Feng^c, Yanxin Li^{a,*}

^aPediatric Translational Medicine Institute, Key Laboratory of Pediatric Hematology and Oncology Ministry of Health, State Key Laboratory of Oncogenes and Related Genes, Department of Hematology & Oncology, Shanghai Children's Medical Center, Shanghai Jiao Tong University School of Medicine, Shanghai, China; ^bState Key Laboratory of Bioorganic and Natural Products Chemistry, Center for Excellence in Molecular Synthesis, Shanghai Institute of Organic Chemistry, Chinese Academy of Sciences, Shanghai, China; ^cState Key Laboratory of Oncogenes and Related Genes, Renji-Med X Clinical Stem Cell Research Center, Ren Ji Hospital, Shanghai Cancer Institute, Shanghai Jiao Tong University School of Medicine, Shanghai, China

Abstract

Tumor relapse is the major cause of treatment failure in childhood acute lymphoblastic leukemia (ALL), yet the underlying mechanisms are still elusive. Here, we demonstrate that *phosphoribosyl pyrophosphate synthetase 2* (*PRPS2*) mutations drive ALL relapse through influencing PRPS1/2 hexamer stability. Ultra-deep sequencing was performed to identify *PRPS2* mutations in ALL samples. The effects of *PRPS2* mutations on cell survival, cell apoptosis, and drug resistance were evaluated. In vitro *PRPS2* enzyme activity and ADP/GDP feedback inhibition of *PRPS* enzyme activity were assessed. Purine metabolites were analyzed by ultra-performance liquid-chromatography tandem mass spectrometry (UPLC-MS/MS). Integrating sequencing data with clinical information, we identified *PRPS2* mutations only in relapsed childhood ALL with thiopurine therapy. Functional *PRPS2* mutations mediated purine metabolism specifically on thiopurine treatment by influencing PRPS1/2 hexamer stability, leading to reduced nucleotide feedback inhibition of *PRPS* activity and enhanced thiopurine resistance. The 3-amino acid V103-G104-E105, the key difference between *PRPS1* and *PRPS2*, insertion in *PRPS2* caused severe steric clash to the interface of *PRPS* hexamer, leading to its low enzyme activity. In addition, we demonstrated that *PRPS2* P173R increased thiopurine resistance in xenograft models. Our work describes a novel mechanism by which *PRPS2* mutants drive childhood ALL relapse and highlights *PRPS2* mutations as biomarkers for relapsed childhood ALL.

Key Words: Drug resistance; Childhood acute lymphoblastic leukemia; *PRPS2*; Purine metabolism; Tumor relapse

* Address correspondence: Yanxin Li, E-mail: liyanxin@scmc.com.cn; or Haizhong Feng, E-mail: Fenghaizhong@sjtu.edu.cn; or Bin-Bing S. Zhou, E-mail: binbing_s_zhou@yahoo.com; or Benshang Li, E-mail: leebenshang@hotmail.com

Conflict of interest: The authors declare that they have no conflict of interest.

This work was supported in part by National Natural Science Foundation of China (81972341, 81900158, 81772663, 81874078, 82072896); Shanghai Municipal Science and Technology Commission (201409002700, 19JC1413500, 21XD1403100) and Shanghai Municipal Education Commission-Gaofeng Clinical Medicine Grant Support (20161310), Pudong New Area Science & Technology Development Fund (PKJ2018-Y47).

Y.L. and H.F. designed and supervised the project. L.S., P.L., D.L., H.S., and Y.L. performed experiments. L.S., B.L., H.F., and Y.L. interpreted the data. L.S., B.L., J.W., B.B.S.Z., H.F., and Y.L. wrote or edited the manuscript. All of the coauthors reviewed the manuscript.

All relevant data are available from the authors. All the data supporting the finding of this study are available within the article and its Supplementary Information files or from the corresponding author on reasonable request.

Blood Science (2023) 5, 39–50

Received July 14, 2022; Accepted October 10, 2022.

<http://dx.doi.org/10.1097/BS9.000000000000139>

Copyright © 2022 The Authors. Published by Wolters Kluwer Health Inc., on behalf of the Chinese Medical Association (CMA) and Institute of Hematology, Chinese Academy of Medical Sciences & Peking Union Medical College (IHCAMS). This is an open-access article distributed under the terms of the Creative Commons Attribution-Non Commercial-No Derivatives License 4.0 (CCBY-NC-ND), where it is permissible to download and share the work provided it is properly cited. The work cannot be changed in any way or used commercially without permission from the journal.

1. INTRODUCTION

Although the treatment outcome for children with acute lymphoblastic leukemia (ALL) has improved substantially with the use of risk-directed treatment and improved supportive care, relapse remains a leading cause of mortality among all childhood ALL.^{1–3} Abnormal purine metabolism is associated with the progression of cancers^{4–7} and thiopurines are among the first line drugs in ALL chemotherapy.^{1,3} Mutations in *phosphoribosyl pyrophosphate synthetase 1* (*PRPS1*), the first rate-limiting and allosteric enzyme in the purine biosynthesis pathway,^{8–10} had been identified to drive drug resistance and childhood ALL relapse by reducing nucleotide feedback inhibition.^{11,12} However, the mechanisms by which purine metabolism regulates ALL relapse are still elusive.

Phosphoribosyl pyrophosphate synthetase 2 (*PRPS2*) encodes another *PRPS* isoform in the purine biosynthesis pathway,^{10,13–16} which shares 95% homology with *PRPS1* amino acid sequence.^{9,17} *PRPS2* was identified as a single rate-limiting enzyme coupling protein and nucleotide biosynthesis in Myc-driven tumorigenesis⁴ and regulated DNA damage¹⁸ and cancer stem cell self-renewal.⁶ Recently, we had implicated that *PRPS2* could be important for thiopurine resistance in Burkitt lymphoma¹⁹ and ALL.¹¹ *PRPS2* forms a complex with *PRPS1* and other 2 *PRPS*-associated proteins.^{9,20,26} However, the functions of *PRPS2* in cancer metabolism and cancer relapse are still poorly understood.

In this study, integrating sequencing data of total 210 matched diagnosis-relapse samples in 2 independent ALL validation cohorts^{11,12} with clinical information from our center, Shanghai Children's Medical Center (SCMC), we identified novel therapy-induced and recurrent relapse-specific mutations in *PRPS2*. Moreover, the functional *PRPS2* mutations specifically regulated drug resistance through influencing *PRPS1/2* hexamer stability, leading to reduced nucleotide feedback inhibition of *PRPS* activity. Our findings demonstrate a novel mechanism by which *PRPS2* mutants drive drug resistance and childhood ALL relapse.

2. MATERIALS AND METHODS

2.1. Whole-exome sequencing and analysis

Whole-exome capture libraries were prepared according to standard protocols using SureSelect Human All Exon 50 and 38 Mb kit (Agilent technologies). Whole-exome sequencing was performed by using the Illumina HiSeq2000 instrument. SNVs/indels were detected as we described previously.¹²

2.2. Cell culture

HEK-293T cells, leukemia Reh, SUP-B15, Jurkat, and Molt4 cell lines were from ATCC (Manassas, Virginia). Reh, SUP-B15, Jurkat, and Molt4 cells were cultured in 10% FBS/RPMI 1640 medium. HEK-293T cells were cultured in 10% FBS/DMEM medium. All cells were incubated at 37 °C in 5% CO₂. All cell lines in this study were authenticated using STR DNA fingerprinting, most recently in October 2017 by Shanghai Biowing Applied Biotechnology Co., Ltd (Shanghai, China), and mycoplasma infection was detected using LookOut Mycoplasma PCR Detection kit (Sigma-Aldrich).

2.3. Stable gene knockout using CRISPR/CAS9

Lenti CRISPR/Cas9 vector was a gift from Feng Zhang (Addgene plasmid #49535).³² gRNAs were designed following the protocol of Zhang laboratory (<http://crispr.mit.edu>). The sequence targeted by *PRPS1* CRISPR is 5'-TTGGTCCTTACCAGGTCTCC-3' and the sequence targeted by *PRPS2* CRISPR is 5'-GGATGATGACGCAATCTTGC-3'.

2.4. Lentivirus production and infection

Human *PRPS1* and *PRPS2* coding regions were cloned into pGV303 Vector (GeneChem, Shanghai, China) and different mutations were constructed using site-directed mutagenesis and confirmed by DNA sequencing. The constructs were transfected with packaging plasmids psPAX₂ and pMD₂G into HEK293T cells using the calcium phosphate method to produce replication-defective virus. The supernatant was harvested 48 hours later and concentrated by 100 kDa column (Amicon purification system, MILLIPORE), and Reh cells were virally transduced with supplemented with 8 µg/mL polybrene (Sigma). The medium was changed 24 hours after infection, and GFP-positive cells were sorted using MoFlo XDP (Beckman Coulter, Brea, CA, US).

2.5. Cell viability and apoptosis assays

Cell viability was determined by using Cell Titer-Glo Luminescent kit (Promega) according to the manufacturer's instructions as we previously described.¹² Briefly, cells were seeded in 96-well plated at 10,000 per well and treated with drugs of different serial dilutions for 72 hours. Then, the Cell Titer-Glo Reagents (50 µL) were added to each well and mixed for 10 min before the luminescent signal was measured using a microplate reader (Biotek, Winooski, Vermont, US). Apoptosis was measured using Annexin V-PE and 7-AAD staining (Annexin V-PE Apoptosis Detection kit, BD Biosciences, Franklin

Lakes, NJ, US) followed by flow cytometry analysis using a FACS (Canto II) as we previously described.³³

2.6. IP and WB

IP and WB were performed as we previously described.³⁴ Cells were lysed in an IP buffer (20 mM Tris-HCl, pH 7.5, 150 mM NaCl, 1 mM EDTA, 2 mM Na₃VO₄, 5 mM NaF, 1% Triton X-100 and protease inhibitor cocktail) at 4°C for 30 minutes. The lysates were centrifuged, and the protein concentrations were determined. Equal amounts of cell lysates were immunoprecipitated with specific antibodies and protein G-agarose beads (Invitrogen, Carlsbad, California). Standard WB was performed with antibodies against γH2AX(S139) (#3522-1, Epitomics, Burlingame, CA, US), PARP (#46D11, Cell Signaling Technology, Danvers, MA, US), Cleaved PARP (Asp214) (D64E10, Cell Signaling Technology, Danvers, MA, US), His-Tag (D3I10, Cell Signaling Technology, Danvers, MA, US), β-actin (I-19, Santa Cruz Biotechnology, Dallas, TX, US), *PRPS2* (NBP1-56666, Novus Biologicals), *PRPS1* (sc-376440, Santa Cruz Biotechnology, Dallas, TX, US), or Flag (MS2, Sigma-Aldrich, Burlington, MA, US) using the Odyssey system (LI-COR Biosciences, Lincoln, NE, US).

2.7. Protein purification

WT or mutants of *PRPS1* and *PRPS2* genes with an N-terminal hexahistidine (6×His) tag were cloned into the pET-28a expression vector. The plasmids were transformed into and expressed in *E. coli* BL21 (DE3) strain (Tiangen). Then, harvested cells pellets were suspended in buffer A [50 mM NaH₂PO₄ (pH 8.0), 1 M NaCl, 15% (Weight/Volume) glycerol, 5 mM 2-mercaptoethanol and 1 mM PMSF] and lysed on ice by sonication before the supernatants were collected by centrifugation. The supernatants were loaded onto a Ni Sepharose FF column (GE Healthcare, Pittsburgh, PA, US) in the AKTA purifier system. The column was washed with buffer A and then eluted with buffer B (Buffer A+500 mM imidazole). We removed imidazole through buffer exchange using G25 desalting columns (GE Healthcare), and assessed protein expression and purity using SDS-PAGE with Coomassie Brilliant Blue R250 staining.

2.8. *PRPS1/2* enzymatic activity and ADP/GDP feedback inhibition assays

PRPS1/2 enzyme activity and ADP/GDP feedback inhibition of *PRPS* enzyme activity were performed using a Kinase-Glo luminescent kinase assay Kit (Promega) according to the manufacturer's instructions as we previously described.¹² In brief, 10 µL purified recombinant WT or mutant *PRPS1* or *PRPS2* with various concentration was incubated in 100 µL of reaction buffer (50 mM Tris, pH 7.5, 10 mM MgCl₂, 1 mM DTT, 500 µM ATP, 500 µM R5P, 2 mM phosphate) at 37°C for 1 hours in a 96-well plate. The reaction was terminated by adding 10 µL Kinase-Glo reagent. In GDP feedback inhibition assay, GDP from 6 to 0.25 µM was added in the reaction buffer.

2.9. Metabolite flux assays

Metabolite flux assays were performed as described previously.¹² Cells were cultured in RPMI 1640 media at a density of 5 × 10⁵/mL. Isotope-labeled [¹³C₂, ¹⁵N] Glycine (Sigma, Cat#489522) or [¹³C₃, ¹⁵N₄] Hypoxanthine (Cambridge Isotope Laboratories, Tewksbury, MA, US, Cat#CNLM-7894-PK) was added to cells then cultured for 2 hours. Cells were then harvested, pelleted and quenched in cold 80% methanol, centrifuged at 12,000 rpm for 10 minutes, and the supernatant was applied for metabolite analysis by AB

SciexQtrap 5500 coupled with Waters Acquity UPLC. IMP synthesis (flux) through de novo purine synthesis pathway was measured by [$^{13}\text{C}_2$, ^{15}N] incorporation into cells (molecular weight peak IMP+3); IMP synthesis (flux) through purine salvage pathway measured by [$^{13}\text{C}_5$, $^{15}\text{N}_4$] incorporation into cells (molecular weight peak IMP+9).

For PRPP measurement, cells were cultured in RPMI 1640 media and then labeled with [$\text{U-}^{13}\text{C}_6$] D-glucose (Cambridge isotope laboratories) for 5 minutes. Cells were then harvested, pelleted and quenched in cold 80% methanol, the newly synthesized PRPP in cells were measured by [$^{13}\text{C}_5$] incorporation into cells (molecular weight peak PRPP+5). For ADP and GDP feedback inhibition test, we first treated cell by 2 mM ADP or 1.5 mM GDP for 24 hours, and then harvested the cells and measured the newly synthesized.

2.10. Thiopurine conversion and thiopurine cytotoxic metabolite assays

Cells were cultured in RPMI 1640 media containing 10 μM 6-MP for 4 hours, then harvested and assayed based on a method modified as described previously.¹² Intracellular accumulation of TIMP, 6-MP metabolites and their derivatives were determined by LC-MS as described previously.¹²

2.11. Structural analysis

Structural analysis of various PRPS2 mutations and the 3AA was based on the crystal structure of human PRPS1 (PDB code, 2HCR).¹⁷ The figures were prepared using PyMol (www.pymol.org).

2.12. Size-exclusion chromatography

A HiPrep 16/60 Sephacryl S-300 HR column (GE) was used to perform size-exclusion chromatography according to the manufacturer's recommendation. Briefly, cell lysates were loaded onto the column and collected at a flow rate of 0.3 mL/min. Then, the sample fractions were analyzed using WB. The standard curve of the elution was plotted against LogMW by using a size-exclusion chromatography calibration marker kit (Sigma) according to the manufacturer's recommendation.

2.13. Immunofluorescence staining

Human PRPS1 or PRPS2 cDNA was cloned into the pcDNA3.1-EGFP or pcDNA3.1-RFP vector, respectively. In pcDNA3.1-EGFP and pcDNA3.1-RFP vectors, the monomeric green fluorescent protein (mEGFP) and the monomeric RFP (mRFP) were derived from hTriGART-mEGFP and pHFGAMS-mOFP (gifts from Dr. Stephen J. Benkovic, the Pennsylvania State University).²⁷ Then, PRPS1-mRFP and PRPS2-mEGFP plasmids were transiently co-transfected into Reh cells cultured in purine-rich media (10% FBS/RPMI 1640 medium) using Lipofectamine 2000 (Invitrogen). Cells were maintained in purine-depleted media (RPMI 1640 medium with dialyzed 5% FBS) for 3 days as reported previously.²⁷ Finally, cells were collected, fixed, and images were produced with a confocal microscope (Leica, Buffalo Grove, Illinois) at X 600 magnification.

2.14. Tumorigenesis studies

White severe combined immunodeficiency (SCID) female mice aged 6–8 weeks (SLAC, Shanghai, China) were used. Mice were randomly divided into 5 per group. In total, 1×10^6 clinical ALL cells were injected into recipients through the tail vein as previously described.³⁵ After 7 days, the mice were treated with the vehicle (PBS) or 0.6 mg/kg 6-MP per day for 10 days.

Mice were euthanized when ALL symptoms developed. All animal experiments were performed in accordance with a protocol approved by Shanghai Jiao Tong University Institutional Animal Care and Use Committee (IACUC).

2.15. Statistics analysis

GraphPad Prism version 5.0 for Windows (GraphPad Software Inc., San Diego, California) was used to perform one-way analysis of variance (ANOVA) with Newman–Keuls post hoc test or an unpaired, 2-tailed Student *t*-test. Relapsed ALL analysis was carried out by Kaplan–Meier analysis and was compared with Newman–Keuls post-test as we previously described.³⁴ A *P* value of less than .05 was considered statistically significant. All data represent the mean \pm SD of 3 independent experiments/samples unless specifically indicated.

3. RESULTS

3.1. PRPS2 mutations are closely associated with drug resistance and childhood ALL relapse

To determine how genetic lesions contribute to the relapse in childhood ALL, we screened our deep sequencing data of 210 paired diagnosis-relapse bone marrow samples in 2 independent ALL validation cohorts with clinical information^{11,12} from our center, SCMC and found 7 relapse-specific PRPS2 mutations in 6 patients ($n = 6$; 6/210, 2.9%) causing A134T, S106I, V48M, R22S, P173R, P173Y, or A175T mutation, respectively (Fig. 1A and Supplemental Table 1, <http://links.lww.com/BS/A50>). Since human PRPS1 exists as a hexamer comprising 3 homodimers,¹⁷ we made a simulated hexamer crystal structure of human PRPS2 based on the reported crystal structure of human PRPS1^{17,21} and then mapped PRPS2 mutations. As shown in Figure 1B, the S106, A134, and A175, but not V48 and R22, residues are at trimer-trimer interface, and the P173 residue is in a turn motif and may be critical to maintain interface helix conformation. Since PRPS2 functions in purine biosynthesis and its mutations are associated with on-treatment relapse, we determined whether mutations in PRPS2 allow for resistance to nucleotide analogs in ALL thiopurine chemotherapy. Ectopic expression of PRPS2 P173R, P173Y, or A175T mutant markedly increased cell resistance to thiopurines (6-MP and 6-TG)³ in Reh ALL cells compared to the empty vector (EV) or PRPS2 wild type (WT) (Fig. 1C and D) whereas the expression of PRPS2 WT, A134T, S106I, V48M, or R22S mutant had minimal or no effects on drug resistance (Fig. 1C and D). In addition, ectopic expression of PRPS2 WT or these mutants had minimal effects on sensitivity to other chemotherapeutics used in clinical ALL treatment (Supplemental Figure 1A, <http://links.lww.com/BS/A50>), such as methotrexate (MTX), L-asparaginase (L-ASP), daunorubicin (DNR), or cytosine arabinoside (Ara-C)²² compared with the EV control. There were no significant effects on cell proliferation expressing PRPS2 WT or mutants compared to the control (Supplemental Figure 1B, <http://links.lww.com/BS/A50>). These results suggest that PRPS2 mutations at P173 and A175 residues are specific for thiopurine resistance.

Thiopurines exert their cytotoxicity primarily through mismatch repair pathway-mediated DNA damage response (DDR) and apoptosis.²³ Drug-resistant PRPS2 P173R, P173Y, and A175T mutations reduced 6-MP-induced cell apoptosis compared to the EV control (Fig. 1E), whereas PRPS2 WT, S106I, and R22S mutations, but not the A134T and V48M mutations, increased cell apoptosis (Fig. 1E). This observation was validated by assessing expression levels of the apoptosis biomarker cleaved poly (ADP-ribose) polymerase (PARP) and the DDR biomarker γ -H2AX (Fig. 1F). We further tested the effects of PRPS2 WT and mutations on cell viability and cell apoptosis in other leukemia cell lines, including SUP-B15, Jurkat, and Molt4, and found the similar results. Overexpression of the

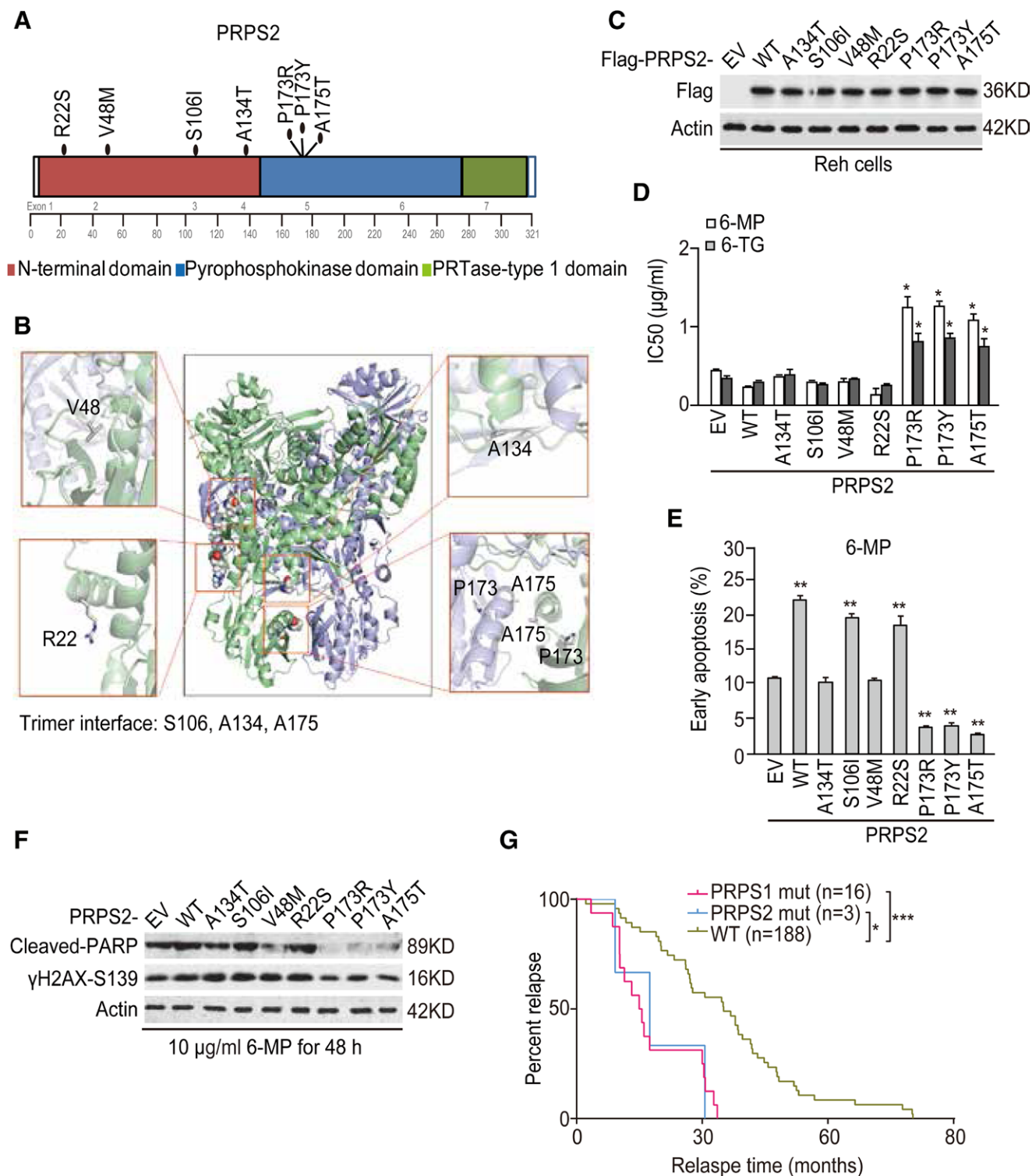


Figure 1. PRPS2 mutations are closely associated with drug resistance and childhood ALL relapse. (A) Schematic diagram showing relapse-specific PRPS2 missense mutations. (B) Mapping the relapse-specific mutant PRPS2 residues onto the simulated crystal structure of the human PRPS2 dimer by tFold showing 1 subunit in cyan and the other in blue. (C) WB of ectopic expression of PRPS2 mutations in Reh cells. (D) Viability of cells with EV, PRPS2 WT, or mutations treated with 6-MP or 6-TG. (E) Early apoptosis analysis. Reh cells were treated with 10 µg/mL 6-MP for 48 h. (F) DNA damage response and apoptosis assays. (G) Kaplan–Meier analysis of childhood ALL relapse with functional PRPS2 or PRPS1 mutations (mut) versus WT. Median relapse time (mo): PRPS2 mut, 17.47; PRPS1 mut, 15.29; WT, 35.10. Data represent the mean ± SD. * $P < .05$, ** $P < .01$, *** $P < .001$, by 2-tailed Student t-tests or log-rank test. ALL = acute lymphoblastic leukemia, EV = empty vector, PRPS2 = phosphoribosyl pyrophosphate synthetase 2, WB = Western blotting, WT = wild type.

drug-resistant PRPS2 P173R, P173Y, or A175T mutant significantly increased cell viability (Supplemental Figure 2A and B, <http://links.lww.com/BS/A50>) and reduced cell apoptosis (Supplemental Figure 2C, <http://links.lww.com/BS/A50>) after

treatment with 6-MP and 6-TG compared with WT PRPS2 and the EV control in the 3 leukemia cell lines. These data support that drug-resistant PRPS2 mutations promote thiopurine resistance by impairing thiopurine-induced DDR and cell apoptosis.

Finally, we checked the treatment and survival of ALL patients with *PRPS2* mutations. Interestingly, all functional *PRPS2* mutations (P173 and A175) were identified in patients with continuous thiopurine (6-MP and/or 6-TG) treatment (Supplemental Figure 3, <http://links.lww.com/BS/A50>), whereas other *PRPS2* mutations were detected in patients after stopping thiopurine treatment. We further performed ultra-deep sequencing of matched samples obtained at diagnosis, remission, and relapse from 2 patients with *PRPS2* A175 or P173 mutation, and found that *PRPS2* A175 or P173 mutation was only identified in the relapse specimen (Supplemental Table 2, <http://links.lww.com/BS/A50>). Then, we examined the relationship of *PRPS2* functional mutations and ALL relapse by the Kaplan–Meier analysis in the 2 cohorts and found a statistically significant shorter relapse time for ALL patients with *PRPS2* mutations (mut) compared with those with WT *PRPS2* and WT *PRPS1* (WT) with a median relapse time 17.47 and 35.10 months, respectively ($P < .05$, Fig. 1G). There was no survival difference between those with *PRPS2* mut and *PRPS1* mut, with a median relapse time 17.47 and 15.29 months, respectively (Fig. 1G). Taken together, our data strongly indicate that *PRPS2* mutations are closely associated with drug resistance and childhood ALL relapse.

For the similar functions of A175 and the P173 residue in a hexamer and drug resistance to 6-MP/6-TG, we selected P173R did the next experiments.

3.2. *PRPS2* P173R mutation regulates PRPS activities

We previously reported that ectopic expression of *PRPS1* WT had some partial thiopurine resistance effect, while *PRPS1* A190T mutant, with constitutive high enzyme activity, had enhanced thiopurine resistance.¹² However, in our current study, the overexpression of *PRPS2* WT did not affect drug resistance compared with the EV control, whereas *PRPS2* P173R mutation significantly enhanced thiopurine drug resistance (Fig. 2A). This observation suggests that *PRPS2* might play different roles from *PRPS1* in purine biosynthesis and thiopurine resistance.

PRPS2 was thought to have lower enzymatic activity than *PRPS1* and not subject to feedback inhibition.⁹ We purified WT and mutant of *PRPS1* and *PRPS2* and performed enzymatic activity assays. As shown in Figure 2B, the enzymatic activity of WT *PRPS2* was significantly lower than that of *PRPS1* WT or A190T mutant, and the activity of *PRPS2* P173R mutant had no marked difference from that of *PRPS2* WT. This result suggests that the drug resistance of *PRPS2* P173R mutant is not directly correlated with *PRPS2* enzymatic activity.

As we and others have demonstrated that PRPS activities are best measured using cell-based assays,^{12,24} we further detected *PRPS1/2* downstream metabolites specific for the de novo and salvage purine pathways (Fig. 2C) by LC-MS with isotope-labeled substrates with or without 6-MP treatment in Reh cells. Consistent with our earlier results,¹² compared to the EV control, ectopic expression of *PRPS1* WT or A190T mutant increased the levels of purine nucleotides in the de novo purine pathway, IMP (+3), IMP (+9), HX, ADP, PRPP, and GDP with or without 6-MP treatment and decreased the levels of cytotoxic molecules (TIMP and TGMP) in the salvage purine pathway under 6-MP treatment (Fig. 2D). In contrast, overexpression of WT *PRPS2* had no significant influence on all purine biosynthesis of intermediates compared with the EV control with or without 6-MP treatment (Fig. 2D). However, only on 6-MP treatment, ectopic expression of *PRPS2* P173R mutant markedly increased the levels of HX, ADP, and GDP and moderately decreased TGMP and TIMP levels compared with the EV control (Fig. 2D). These data suggest again that *PRPS2* P173R mutation specifically mediates therapy-induced purine metabolism and its functions may be different from *PRPS1* WT and A190T mutant.¹²

We further performed nucleotide feedback inhibition of PRPS activity with ADP or GDP treatment in Reh cells.^{12,24} As shown in Figure 2E, ADP/GDP treatment inhibited the labeled PRPP production in the cells expressing *PRPS1* WT but not the A190T mutant as we previously reported that *PRPS1* A190T mutation impairs the nucleotide feedback inhibition of PRPS activities.¹² *PRPS2* WT overexpression had no effect on the labeled PRPP production after ADP or GDP treatment, whereas ectopic expression of *PRPS2* P173R mutant significantly increased PRPP production (Fig. 2E), suggesting that *PRPS2* P173R mutation also affects the nucleotide feedback inhibition of cellular PRPS enzymatic activity. This is further supported by effects of ectopic expression of *PRPS2* P173R mutant on purine derivative hypoxanthine (HX)¹² and GART inhibitor lometrexol^{12,25} treatment-induced 6-MP resistance. HX treatment enhanced 6-MP resistance in all the indicated cells, including the cells expressing an EV control (Fig. 2F). However, as in WT or A190T mutant *PRPS1* cells, lometrexol treatment enhanced 6-MP resistance in the cells expressing *PRPS2* P173R mutant but not WT *PRPS2* or the EV control (Fig. 2G). These data suggest that *PRPS2* P173R mutation resembles *PRPS1* A190T mutation to cause defects in the nucleotide feedback inhibition of PRPS activities in thiopurine resistance.

3.3. *PRPS2* is critical for nucleotide feedback inhibition of PRPS activity

To demonstrate the function of *PRPS2* in nucleotide feedback inhibition of PRPS activity, we established *PRPS2* KO and *PRPS1* KO cell lines using CRISPR/Cas9 technology. Knockout of *PRPS1* or *PRPS2* significantly caused Reh cell sensitivity to 6-MP treatment (Fig. 3A and B) and promoted cell apoptosis (Fig. 3C), suggesting that both *PRPS1* and *PRPS2* are important for thiopurine resistance in childhood ALL.

Next, we determined nucleotide feedback inhibition of PRPS activity with ADP or GDP treatment in Reh cells with *PRPS1* KO or *PRPS2* KO as we described previously.^{12,24} Both *PRPS1* KO and *PRPS2* KO markedly reduced the PRPS activity (Fig. 3D). However, ADP and GDP treatment significantly reduced PRPP production in *PRPS2* KO and control cells but not *PRPS1* KO cells (Fig. 3D). This shows that *PRPS2* is critical for nucleotide feedback inhibition of PRPS activity.

The dNTP pools are affected by the metabolites of the purine synthesis and regulate genomic stability.^{5,12} To support our above observation, we measured the dNTP pools by metabolite flux in the indicated Reh cells (Fig. 3E). Deletion of *PRPS1* or *PRPS2* markedly reduced dNTP pools whereas there was no difference between *PRPS1* KO and *PRPS2* KO (Fig. 3E). Taken together, these results demonstrate that *PRPS1* and *PRPS2* have different functions in regulating PRPS activity.

3.4. The 3-amino acid V103-G104-E105 insertion in *PRPS2* significantly decreases its PRPS activity

To determine the functional difference, we compared the amino acid sequences of human *PRPS1* and *PRPS2* and found that a sequence difference is the 3-amino acid V103-G104-E105 (3AA, VGE) of *PRPS2* (Fig. 4A and Supplemental Figure 4A, <http://links.lww.com/BS/A50>). The *PRPS1* hexamer crystal structure shows that the loop of ₉₈-DKKDKSRAPISAK-₁₁₀ is critical for the compact hexamer formation in *PRPS1* (Supplemental Figure, 4B <http://links.lww.com/BS/A50>) and the 3AA (VGE) insertion in *PRPS2* caused severe steric clash to the interface of 2 trimers of the hexamer formed by a *PRPS1* trimer and a simulated *PRPS2* trimer (Fig. 4B).

To test our hypothesis, we swapped the 3AA between *PRPS2* and *PRPS1*: inserting the nucleotides encoding the 3AA into the

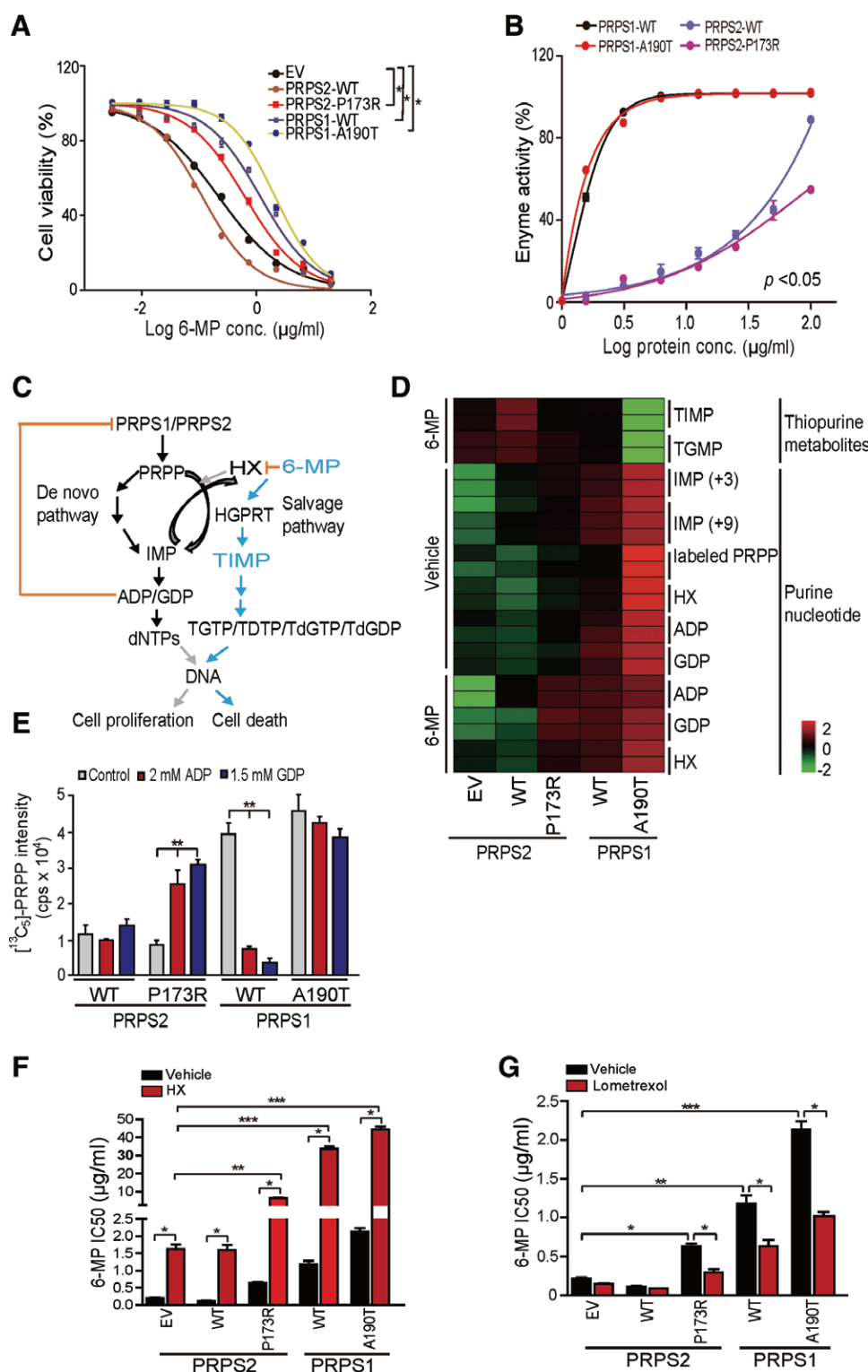


Figure 2. PRPS2 P173R mutation regulates PRPS activities. (A) Effects of overexpression of PRPS2 WT, KO, P173R mutant, PRPS1 WT, A190T mutant, or an EV on cell viability at increasing concentrations of 6-MP. (B) Enzyme activities were analyzed using a Kinase-Glo Luminescent Kinase Assay kit. (C) Diagram illustrating the de novo purine biosynthesis pathway and the purine salvage pathway. (D) Heatmap showing thiopurine metabolites TIMP and TGMP, and metabolomics analysis of ADP, GDP, de novo purine flux, purine salvage flux in Reh cells treated with or without 6-MP. (E) ADP/GDP feedback inhibition of PRPS activity measured by [$^{13}\text{C}_5$]-PRPP in Reh cells. (F and G) Cell viability assays of Reh cells with or without HX or GART inhibitor lometrexol treatment. Data represent the mean \pm SD. * $P < .05$, ** $P < .01$, *** $P < .001$, by 2-tailed Student t-tests. EV = empty vector, KO = knockout, PRPS2 = phosphoribosyl pyrophosphate synthetase 2, WT = wild type.

full length of *PRPS1* (named PRPS1^{+3AA}), or deleting the nucleotides from *PRPS2* (named PRPS2^{-3AA}) (Fig. 4C). PRPS1^{+3AA} mutation significantly attenuated cell resistance to 6-MP

compared to PRPS1 WT, whereas PRPS2^{-3AA} mutant increased cell resistance compared with PRPS2 WT. We purified PRPS1^{+3AA} and PRPS2^{-3AA} mutant proteins and found that PRPS1^{+3AA}

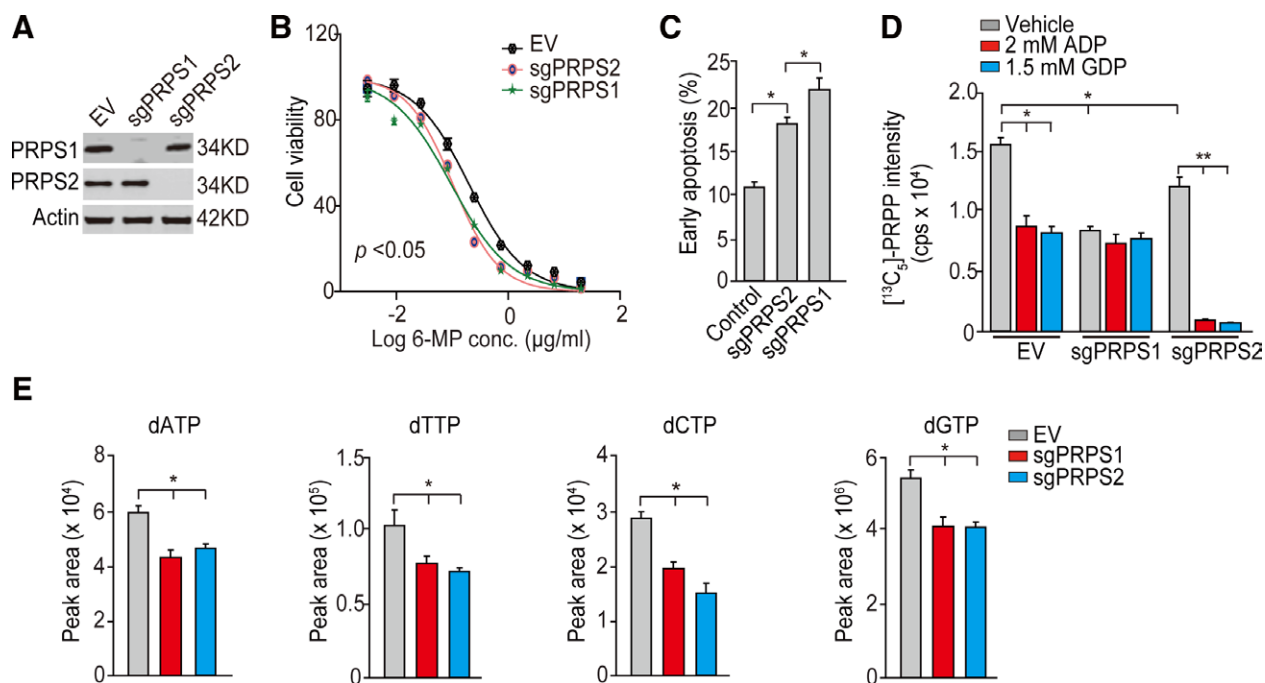


Figure 3. PRPS2 is critical for nucleotide feedback inhibition of PRPS activity. (A) WB of PRPS1 KO and PRPS2 KO. (B) Effects of PRPS2 KO and PRPS1 KO on Reh cell viability at increasing concentrations of 6-MP. (C) Early apoptosis assays. Reh cells were treated with 10 μ M 6-MP for 48h. (D) Nucleotide feedback inhibition of PRPS enzyme activity measured by [¹³C₅]-PRPP in Reh cells with PRPS1 KO, PRPS2 KO, or an EV control. (E) dNTP pool analysis in Reh cells. Data represent the mean \pm SD. * $P < .05$, ** $P < .01$, by 2-tailed Student t-tests. KO = knockout, PRPS2 = phosphoribosyl pyrophosphatase 2, WB = Western blotting, WT = wild type.

mutant markedly reduced PRPS enzyme activity in comparison with PRPS1 WT, whereas PRPS2-3AA mutant has higher activity than PRPS2 WT (Fig. 4E). These data support that the 3AA is critical for PRPS activity.

Next, we detected the effects of the 3AA on PRPS downstream metabolites in Reh cells. As shown in Figure 4F, compared to WT PRPS1, ectopic expression of PRPS1^{+3AA} mutant significantly reduced levels of PRPP, ADP, GDP, and HX and increased TGMP and TIMP levels in Reh cells with or without 6-MP treatment. On the contrast, overexpression of PRPS2^{-3AA} mutant significantly increased HX levels in cells without 6-MP treatment and ADP, GDP levels in 6-MP-treated cells compared with PRPS2 WT (Fig. 4F). PRPS2^{-3AA} mutation also reduced TGMP and TIMP levels in cells with 6-MP treatment (Fig. 4F). These data support that the 3AA in PRPS2 is critical for its functional difference from PRPS1.

We further investigated the effects of 2 mutants on nucleotide feedback inhibition of PRPS activity with ADP or GDP treatment. As shown in Figure 4G, ectopic expression of PRPS1^{+3AA} mutant markedly inhibited PRPP production compared with PRPS1 WT, whereas PRPS2^{-3AA} overexpression significantly increased PRPP production compared with PRPS2 WT. ADP and GDP treatment significantly inhibited PRPP production in Reh cells expressing WT PRPS1 or PRPS2^{-3AA} mutant but not in the cells expressing WT PRPS2 or PRPS1^{+3AA} mutant (Fig. 4G). These data further suggests that the 3AA is critical for nucleotide feedback regulation of PRPS activity.

We also tested the effects of insertion of the 3AA into PRPS1 A190T mutant or deletion of the 3AA in PRPS2 P173R mutant on 6-MP resistance and PRPS enzyme activity. Insertion of the 3AA into PRPS1 A190T mutant reversed A190T mutant's drug resistance (Fig. 4H). In contrast, deletion of the 3AA in PRPS2 P173R mutant further enhanced P173R mutant's drug resistance (Fig. 4H). On the other hand, insertion of the 3AA decreased PRPS1 A190T mutant's activity, while remained insensitive to GDP feedback inhibition (Fig. 4I). Deletion of

the 3AA in PRPS2 P173R mutant increased P173R mutant's activity, while gaining sensitivity to GDP feedback inhibition (Fig. 4I). Taken together, these data demonstrate that the 3AA in PRPS2 is critical for its activity and feedback regulation of PRPS activity.

3.5. Thiopurine resistance of PRPS2 P173R mutation depends on PRPS1 expression

Since PRPS1 and PRPS2 are required for purine biosynthesis in ALL cells and they might form complex with other 2 PRPS-associated proteins inside the cell,^{20,26} we hypothesized that higher PRPS cellular activity and the drug resistance of PRPS2 P173R mutant might be related to its interaction with PRPS1 under pathological conditions. To test our hypothesis, we first determined the drug resistance of PRPS1 KO Reh cells expressing PRPS2 WT or P173R mutant and PRPS2 KO Reh cells expressing PRPS1 WT or A190T mutant (Fig. 5A). Compared to the control in Reh cells, PRPS1 KO markedly decreased 6-MP resistance of the cells expressing PRPS2 WT, P173R mutant, or an EV control, whereas PRPS2 KO significantly increased 6-MP resistance of the cells expressing PRPS1 WT and A190T mutant (Fig. 5B). These data suggest that PRPS1 is required for thiopurine resistance of PRPS2 P173R mutation.

Next, we assessed the effects of PRPS2 or PRPS1 KO on PRPS1 and PRPS2 mutants-mediated PRPS downstream metabolites by LC-MS with isotope-labeled substrates. Compared with the control, PRPS1 KO inhibited upregulation of ADP and GDP and downregulation of TIMP and TGMP by PRPS2 P173R mutant but not PRPS2 WT on 6-MP treatment (Fig. 5C). PRPS2 KO further enhanced upregulation of PRPP, ADP, GDP, HX, and downregulation of TGMP and TIMP by PRPS1 WT and P173R mutant with or without 6-MP treatment. These data further support that thiopurine resistance of PRPS2 P173R mutation depends on PRPS1 expression.

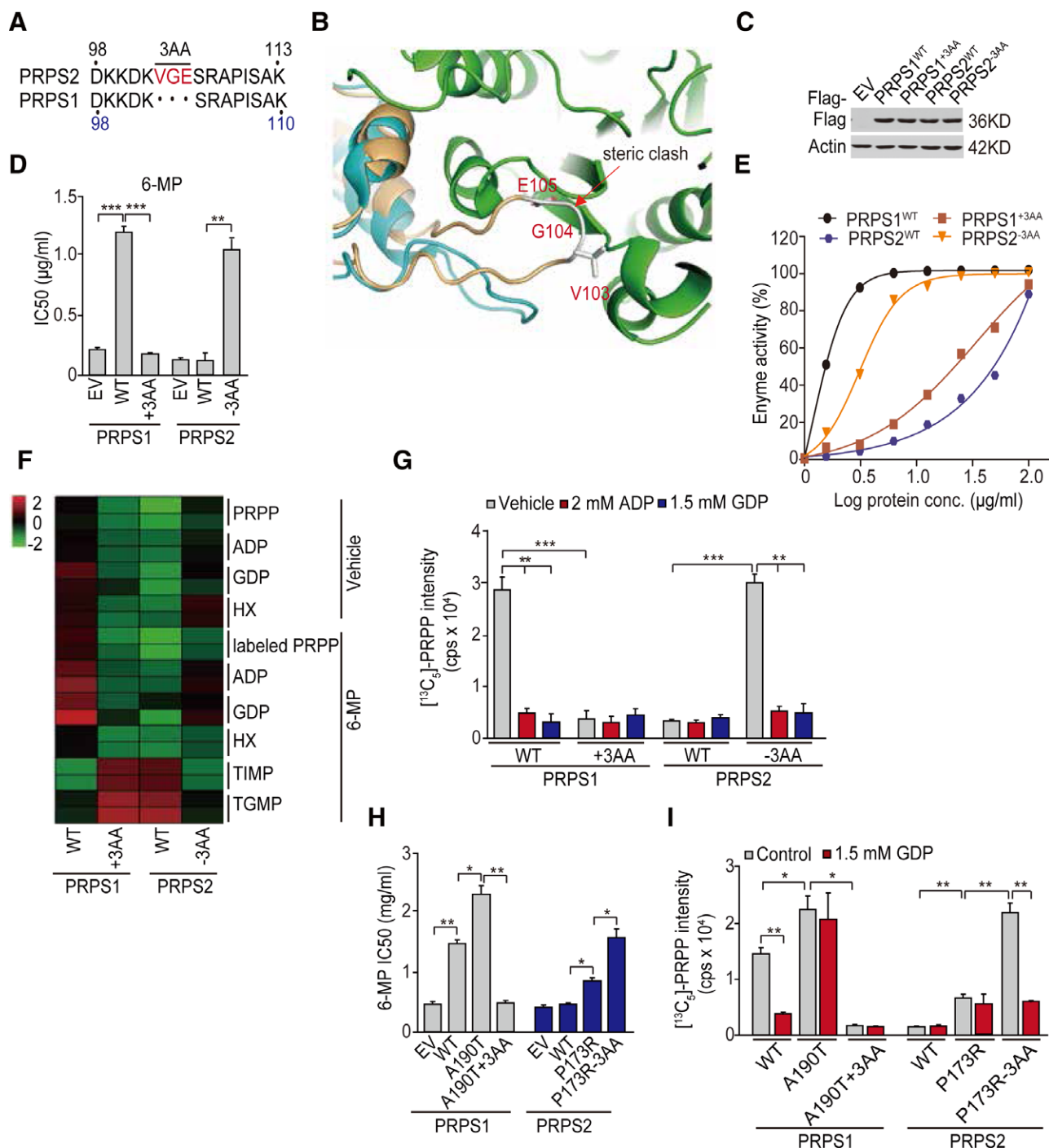


Figure 4. The 3-amino acid V103-G104-E105 insertion in PRPS2 significantly decreases its PRPS activity. (A) The sequence alignment of human PRPS1 and PRPS2 and the 3AA loop in PRPS2. (B) The loop of 98-DKKDKSRAPISAK-110 contributes the compact hexamer formation in PRPS1 in Supplemental Figure 4B, <http://links.lww.com/BS/A50> and the elongated loop in PRPS2 by 103-VGE-105 insertion potentially causes severe steric clash to the interface of 2 trimers of PRPS hexamer. Cyan and green, PRPS1 hexamer (3efh); light-orange, predicted PRPS2-3AA structure. (C) WB of overexpression of PRPS1 WT, +3AA mutant (the 3AA loop was inserted in PRPS1 WT), PRPS2 WT, -3AA mutant (the 3AA loop was deleted in PRPS2 WT). (D) Effects on cell viability treated with 6-MP. (E) Enzyme activities of PRPS1 WT, PRPS1 +3AA mutant, PRPS2 WT, and PRPS2-3AA mutant were analyzed. (F) Heatmap showing effects of PRPS1 +3AA or PRPS2-3AA mutant expression on thiopurine metabolites and metabolomics analysis with or without 6-MP treatment. (G) Effects of 3AA deletion in PRPS2 or 3AA insertion in PRPS1 on nucleotide feedback inhibition of PRPS enzyme activity. (H and I) Effects of deletion or insertion of the 3AA in PRPS1-A190T or PRPS2-P173R mutant on cell viabilities (H) and nucleotide feedback inhibition of PRPS enzyme activity (I) in Reh cells. Data represent the mean \pm SD. * $P < .05$, ** $P < .01$, *** $P < 0.001$, by 2-tailed Student t-tests. EV = empty vector, KO = knockout, PRPS2 = phosphoribosyl pyrophosphate synthetase 2, WT = wild type.

To further demonstrate whether PRPS2 P173R mutation affects the activity of the PRPS1/2 complex, we co-expressed PRPS2 WT or P173R mutant and PRPS1 WT to the

same levels in *Escherichia coli* cells and purified PRPS1/2 and PRPS1/PRPS2-P173R complex, respectively (Fig. 5D). The enzymatic activity of the PRPS1/2 complex is lower than

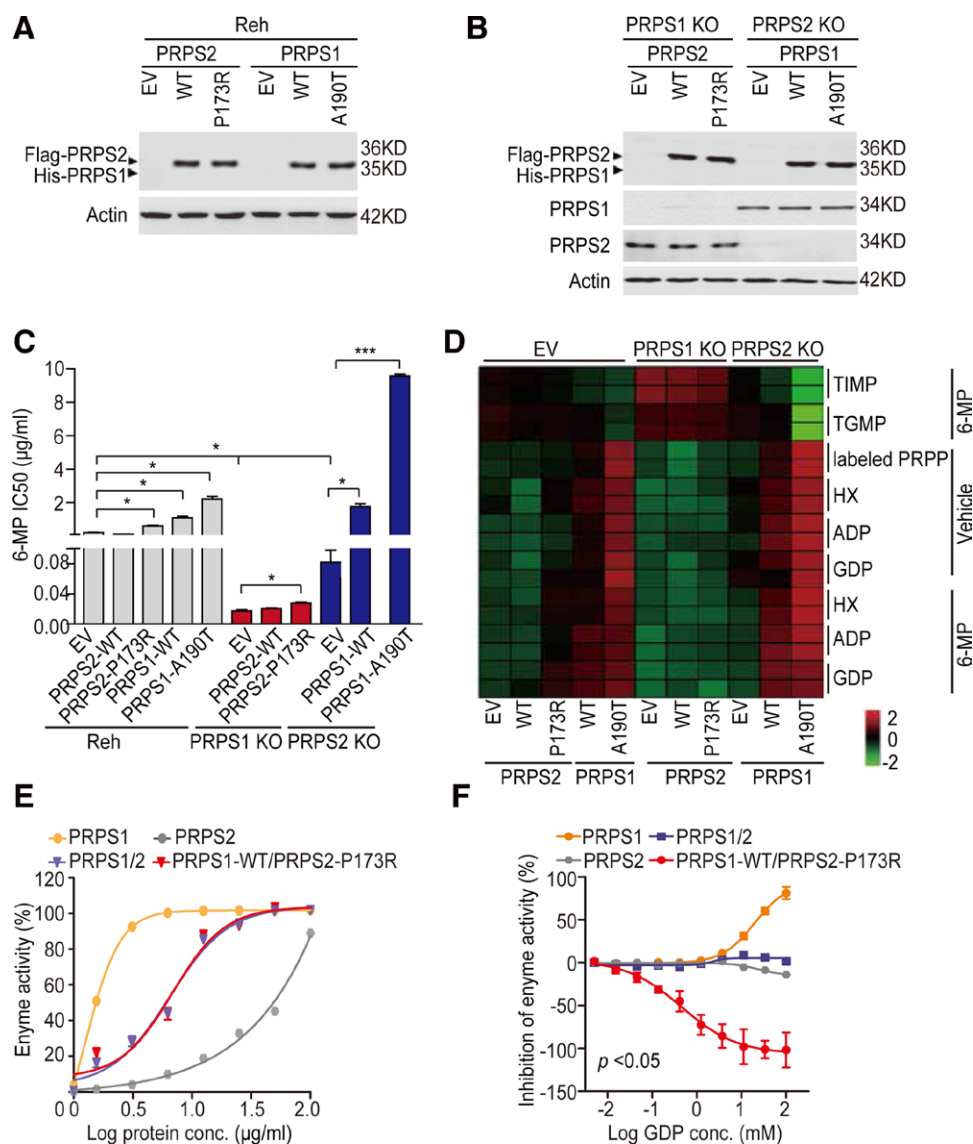


Figure 5. Thiopurine resistance of PRPS2 P173R mutation depends on PRPS1 expression. (A and B) WB of overexpressing PRPS2 WT or P173R mutant and PRPS1 WT or A190T mutant in Reh cells with (A) or without PRPS1 KO or PRPS2 KO (B) compared with EV controls. (C) Effects of PRPS1 KO or PRPS2 KO on viabilities of cells expressing PRPS2 WT, P173R mutant, PRPS1 WT or A190T mutant in Reh cells. (D) Heatmap showing the impact of PRPS1 KO or PRPS2 KO on thiopurine metabolites and metabolomics analysis in the cells from (C). (E) Enzyme activity assays of PRPS1, PRPS2, PRPS1/2 (the complex of PRPS1 WT and PRPS2 WT), PRPS1-WT/PRPS2-P173R (the complex of PRPS1 WT and PRPS2-P173R mutation). (F) In vitro GDP feedback inhibition of PRPS enzyme activity. Data represent the mean \pm SD. * $P < .05$. *** $P < .001$. P values were calculated using 2-tailed Student t -tests. EV = empty vector, KO = knockout, PRPS2 = phosphoribosyl pyrophosphate synthetase 2, WT = wild type.

that of PRPS1 alone but markedly higher than that of PRPS2. On the other hand, the activity of the PRPS1/PRPS2-P173R complex is similar to that of PRPS1/2 (Fig. 5D), supporting that thiopurine resistance of PRPS2 P173R mutation is not due to its enzyme activity. We further investigated the effect of P173R mutation on the nucleotide feedback inhibition of PRPS activity with GDP treatment. Consistent with our previous report,¹² GDP treatment significantly increased the nucleotide feedback inhibition of PRPS activity of purified PRPS1 (Fig. 5E). While there were no effects on the enzyme activities of purified PRPS2 and PRPS1/2 with GDP treatment, the GDP treatment significantly reduced the nucleotide feedback inhibition of PRPS activity of the purified complex of PRPS1/PRPS2-P173R (Fig. 5E). Taken together, our data suggest that thiopurine resistance of PRPS2 P173R mutation depends on PRPS1 in ALL cells.

3.6. PRPS2 P173R mutation influences PRPS hexamer stability

Our simulated hexamer crystal structure of human PRPS2 indicated that the P173 residue in a turn motif may be critical to maintain interface helix conformation and hexamer stability. To determine this observation, we performed immunoprecipitation (IP)-WB analysis and immunofluorescence (IF) staining to examine the effects of the P173R mutant on the interaction and co-localization of PRPS1 and PRPS2 in Reh cells. Compared to PRPS2 WT, nonfunctional S106I and R22S mutants, P173R mutation markedly inhibited its association with PRPS1 in Reh cells (Fig. 6A).

It has been previously demonstrated that PRPS1 and PRPS2 form clusters with other 4 enzymes in the purine de novo pathway in cells.²⁷ To assess whether P173R mutation influences the cluster formation of PRPS enzymes, red fluorescent

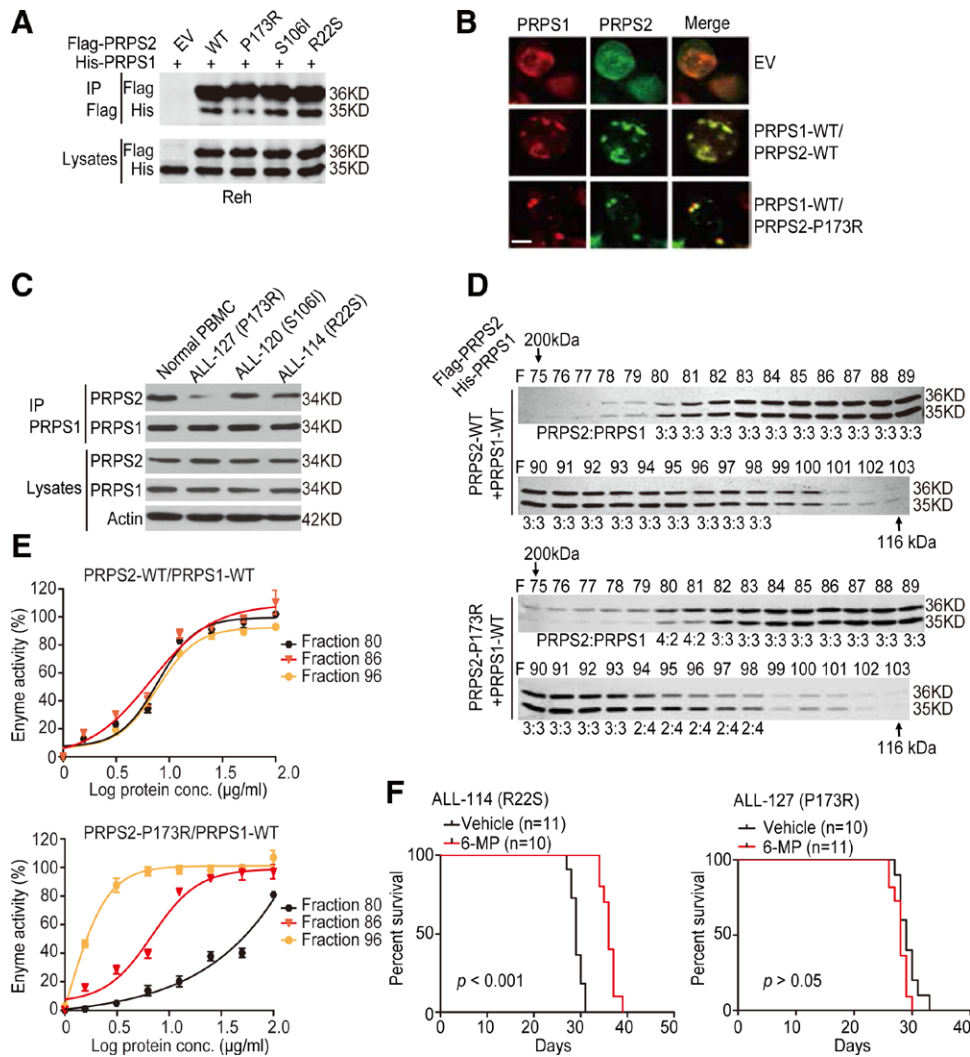


Figure 6. PRPS2 P173R mutation influences PRPS hexamer stability and drug resistance in vivo. (A) IP and WB of binding of PRPS1 with PRPS2 WT or mutations in Reh cells. (B) Immunofluorescence staining of PRPS1-WT co-localization with PRPS2 WT or PRPS2-P173R mutation in Reh cells. Bar, 25 μ m. (C) IP and WB of binding of PRPS1 with PRPS2 WT or mutations in normal PBMC or patient specimens. (D) Purified His-tagged PRPS1 WT complex with Flag-tagged PRPS2 WT or P173R mutation in Reh cells. Fractionation was performed on a size-exclusion column. The indicated fractions were used for the WB assays. Intensity ratios of PRPS2 vs PRPS1 were calculated using NIH ImageJ software. (E) Enzyme activity assays of the fractions in (D) with PRPS2-WT/PRPS1-WT or PRPS2-P173R/PRPS1-WT. (F) Kaplan–Meier analyses of survival of mice engrafted with clinical ALL specimens ALL-114 (PRPS2 R22S mutation) or ALL-127 (PRPS2 P173R mutation) treated with or without 6-MP. After 5 d, mice were treated with or without 0.6 mg/kg 6-MP on Monday, Wednesday, and Friday, for 2 wks. Median survival in WT (in d): vehicle, 29; 6-MP, 36; in P173R, vehicle, 29; 6-MP, 28. The *P* value was calculated by the log-rank test. ALL = acute lymphoblastic leukemia, EV = empty vector, IP = immunoprecipitation, PRPS2 = phosphoribosyl pyrophosphate synthetase 2, WB = Western blotting, WT = wild type.

protein (RFP)-fused PRPS1 WT was transiently co-infected with EGFP-fused PRPS2 WT or P173R mutant into Reh cells, and then cells were cultured in purine-depleted medium for 3 days as described previously.²⁷ As shown in Figure 6B, while PRPS2 WT co-localized with PRPS1 within clusters, the PRPS2 P173R mutant was only partially co-localized with PRPS1 within clusters, supporting that P173R mutation influences the stability of its complex. This observation was further validated by IP and IB analyses in normal peripheral blood mononuclear cells (PBMC) and clinical ALL specimens with PRPS2 mutations. As shown in Figure 6C, compared to normal PBMC control, the functional P173R mutation of PRPS2 but not the nonfunctional S106I and R22S mutations decreased PRPS2 protein binding to PRPS1.

Next, to further reveal how PRPS2 P173R mutation influences the stability of the PRPS1/2 complex, we co-expressed His-tagged PRPS1 WT with Flag-tagged PRPS2 WT or P173R mutant in Reh cells, and performed the size-exclusion chromatography assay as described previously.⁵ As PRPS hexamers and monomers have been detected in human cancer cells,

we collected all the fractions eluted as previously described.⁵ As shown in Figure 6D, Flag-tagged PRPS2 WT or the P173R mutant with His-tagged PRPS1 was detected only in fractions 75–103 that co-eluted with a molecular weight around 200 kDa (according to the molecular weight calibration standard), suggesting that PRPS1 and PRPS2 WT or P173R mutant mainly form hexamers in Reh cells. Quantitative western blot analysis of PRPS1 and PRPS2 relative amounts suggested that the composition of WT PRPS1 and PRPS2 formed stable hexamer complex at a (PRPS2)₃:(PRPS1)₃ ratio, but PRPS2 P173R mutant formed hexamers with WT PRPS1 at ratios of 4:2, 3:3, and 2:4 (Fig. 6D), implicating changes in complex equilibrium and potential weakening of PRPS1 and PRPS2 interaction within hexamer complex. We further collected 3 fractions with PRPS2-WT/PRPS1-WT or PRPS2-P173R/PRPS1-WT and performed enzyme activity assays. As shown in Figure 6E, all the fractions with the same ratio of PRPS2 WT versus PRPS1 WT had similar enzymatic kinetic curves and there was no difference for their enzyme activity. Compared to the complex fraction 86

with a 3:3 ratios of PRPS2 P173R versus PRPS1 WT, the complex fraction 80 with a 4:2 ratio showed lower enzyme activity but the complex fraction 96 with a 2:4 ratio had higher enzyme activity. Taken together, these data demonstrate that *PRPSR* P173R mutation weakens PRPS hexamer stability and increases thiopurine resistance.

To evaluate the *in vivo* drug resistance effect of *PRPS2* P173R mutation, we employed an ALL xenograft model. Clinical ALL specimens, ALL-114 with nonfunctional R22S mutation and ALL-127 with P173R mutation were separately implanted into the immunocompromised mice with intravenous tail injection. The effects of P173R mutation on ALL tumorigenesis with or without 6-MP treatment were assessed. As shown in Figure 6F, 6-MP treatment significantly increased the survival of animals bearing R22S mutation xenografts (ALL-114) but did not affect the survival of those bearing P173R mutant xenografts (ALL-127), providing *in vivo* evidence supporting the role of *PRPS2* P173R mutation in ALL drug resistance and tumor relapse. Taken together, these data demonstrate that *PRPS2* P173R mutation influences PRPS1/2 hexamer stability and reduces nucleotide feedback inhibition of PRPS activity, leading to abnormal drug resistance and ALL relapse.

4. DISCUSSION

Metabolism is a hallmark for cancer,²⁸ yet the mechanisms by which abnormal metabolism causes drug resistance and tumor relapse are still unclear. Herein, we identified thiopurine therapy-induced PRPS2 mutations as new drivers of drug resistance and ALL relapse. Our study not only demonstrate a novel mechanism by which *PRPS2* mutations induce ALL relapse, but also reveals previously unknown regulation of PRPS2 enzymatic activity.

This study identified and validated the first purine biosynthesis rate-limiting enzyme PRPS2 mutants as new regulators of thiopurine resistance and childhood ALL relapse. PRPS2 was early characterized as a purine biosynthesis enzyme.¹⁵ Later PRPS2 was found as a rate-limiting enzyme of coupling protein and nucleotide biosynthesis.⁴ PRPS2-mediated purine metabolism was also related with tumor glucose deprivation or hypoxia,⁵ innate immune response,¹⁸ and maintenance of brain tumor initiating cells.⁶ However, its roles in drug resistance and tumor relapse are still unknown. Here we integrated the sequencing data of total 210 matched diagnosis-relapse samples in 2 independent ALL validation cohorts with clinical information from our center and identified PRPS2 mutations (2.8%, 3/107 in 2015 SCMC cohort, and 2.9%, 3/103 in 2020 SCMC cohort) as new drivers of therapy resistance and ALL relapse. The overall frequency was lower than PRPS1 (13%, 18/138 in 2015 SCMC cohort, and 3.9%, 4/103 in 2020 SCMC cohort). In addition, there were no patient with both PRPS1 and PRPS2 mutation. So, it suggested that the functional PRPS2 mutations were prognostic factor for ALL relapse. Thus, we reveal a new function of PRPS2, providing a rationale for developing therapeutic strategies to overcome thiopurine resistance in the clinic.

Although PRPS1 and PRPS2 are 2 isoforms in human PRPS family with 95% amino acid sequence identity and can form a complex,^{9,17,29,30} their functional difference is poorly characterized. As far as we know, we were the first to identify that the 3-amino acid V103-G104-E105 in PRPS2 is critical for its PRPS activity. Using genetic approaches, we demonstrated that exchanging the 3AA could shift the enzymatic activity, allosteric regulation, the nucleotide feedback inhibition of PRPS activities and drug resistance between PRPS1 and PRPS2. The 3AA (VGE) insertion in PRPS2 caused severe steric clash to the interface of PRPS hexamer, leading to its low enzyme activity. We found only PRPS2 P173R mutation without PRPS1 was sensitive to thiopurine. That means the main function of PRPS2 P173R mutation was regulation of the nucleotide feedback inhibition of PRPS

activities. The PRPS2 P173 residue was in a turn motif and may be critical to maintain interface helix conformation. PRPS2 P173R mutation caused the hexamer instability, reduced the nucleotide feedback inhibition of PRPS activities to induce drug resistance. The molecular insight of this unique observation warrants further investigation.

Our finding demonstrates that PRPS hexamer stability defect could cause drug resistance and tumor relapse. PRPS2 and PRPS1 form complexes with other 2 phosphoribosyl pyrophosphate synthetase associated proteins (PAP39 and PAP41),^{26,27,31} and the complex stability is critical for PRPS enzymatic activity.⁵ For example, PRPS1 and PRPS2 formed hexamer and mediates nucleotide synthesis to maintain glioma tumor cell growth and survival.⁵ AMPK-dependent phosphorylation of PRPS1 led to conversion of PRPS1/2 hexamers to monomers, thereby inhibiting PRPS1/2 activity and nucleic acid synthesis in response to energy stress.⁵ As we know, we are the first to identify that PRPS2 mutation regulates PRPS1/PRPS2 hexamer stability and the P173 mutation leads to thiopurine resistance and ALL relapse in clinic. Our data are in line of the previous findings and further support the importance of PRPS hexamer.

Our work identified new drivers in drug resistance and ALL relapse and demonstrate a novel mechanism by *PRPS2* mutation impairs PRPS hexamer stability, leading to reduced nucleotide feedback inhibition of PRPS activity. Furthermore, our study identified *PRPS2* mutations as new clinical diagnosis markers and potential therapeutic targets in childhood ALL relapse.

ACKNOWLEDGMENTS

This work was supported in part by National Natural Science Foundation of China (81972341, 81900158, 81470315, 81874078, 82072896); Shanghai Municipal Science and Technology Commission (201409002700,19JC1413500, 21XD1403100) and Shanghai Municipal Education Commission-Gaofeng Clinical Medicine Grant Support (20161310), Pudong New Area Science & Technology Development Fund (PKJ2018-Y47), Collaborative Innovation Center for Translational Medicine at Shanghai Jiao Tong University School of Medicine fund TM201502.

We thank Dr. Stephen J. Benkovic in the Pennsylvania State University for kindly providing hTriGART-mEGFP and pHFGAMS-mOFF.

REFERENCES

- Hunger SP, Mullighan CG. Acute lymphoblastic leukemia in children. *N Engl J Med* 2015;373:1541–1552.
- Inaba H, Greaves M, Mullighan CG. Acute lymphoblastic leukaemia. *Lancet* 2013;381:1943–1955.
- Pui CH, Carroll WL, Meshinchi S, Arceci RJ. Biology, risk stratification, and therapy of pediatric acute leukemias: an update. *J Clin Oncol* 2011;29:551–565.
- Cunningham JT, Moreno MV, Lodi A, Ronen SM, Ruggero D. Protein and nucleotide biosynthesis are coupled by a single rate-limiting enzyme, PRPS2, to drive cancer. *Cell* 2014;157:1088–1103.
- Qian X, Li X, Tan L, et al. Conversion of PRPS hexamer to monomer by AMPK-mediated phosphorylation inhibits nucleotide synthesis in response to energy stress. *Cancer Disc* 2018;8:94–107.
- Wang X, Yang K, Xie Q, et al. Purine synthesis promotes maintenance of brain tumor initiating cells in glioma. *Nat Neurosci* 2017;20:661–673.
- Zhou W, Yao Y, Scott AJ, et al. Purine metabolism regulates DNA repair and therapy resistance in glioblastoma. *Nat Commun* 2020;11:3811.
- Becker MA, Kim M. Regulation of purine synthesis de novo in human fibroblasts by purine nucleotides and phosphoribosylpyrophosphate. *J Biol Chem* 1987;262:14531–14537.
- Nosal JM, Switzer RL, Becker MA. Overexpression, purification, and characterization of recombinant human 5-phosphoribosyl-1-pyrophosphate synthetase isozymes I and II. *J Biol Chem* 1993;268:10168–10175.
- Wyngaarden JB. Regulation of purine biosynthesis and turnover. *Adv Enzyme Regul* 1976;14:25–42.

11. Li B, Brady SW, Ma X, et al. a) Therapy-induced mutations drive the genomic landscape of relapsed acute lymphoblastic leukemia. *Blood* 2020;135:41–55.
12. Li B, Li H, Bai Y, et al. Negative feedback-defective PRPS1 mutants drive thiopurine resistance in relapsed childhood ALL. *Nat Med* 2015;21:563–571.
13. Gerhart J. From feedback inhibition to allostery: the enduring example of aspartate transcarbamoylase. *FEBS J* 2014;281:612–620.
14. Hove-Jensen B, Andersen KR, Kilstrup M, Martinussen J, Switzer RL, Willemoes M. Phosphoribosyl diphosphate (PRPP): biosynthesis, enzymology, utilization, and metabolic significance. *Microbiol Mol Biol Rev* 2017;81:e00040-16.
15. Taira M, Ishijima S, Kita K, Yamada K, Iizasa T, Tatibana M. Nucleotide and deduced amino acid sequences of two distinct cDNAs for rat phosphoribosylpyrophosphate synthetase. *J Biol Chem* 1987;262:14867–14870.
16. Tatibana M, Kita K, Taira M, et al. Mammalian phosphoribosyl-pyrophosphate synthetase. *Adv Enzyme Regul* 1995;35:229–249.
17. Li S, Lu Y, Peng B, Ding J. Crystal structure of human phosphoribosylpyrophosphate synthetase 1 reveals a novel allosteric site. *Biochem J* 2007;401:39–47.
18. Liu R, Li J, Shao J, et al. Innate immune response orchestrates phosphoribosyl pyrophosphate synthetases to support DNA repair. *Cell Metab* 2021;33:2076–2089.e9.
19. Li T, Song L, Zhang Y, et al. b) Molecular mechanism of c-Myc and PRPS1/2 against thiopurine resistance in Burkitt's lymphoma. *J Cell Mol Med* 2020;24:6704–6715.
20. Kita K, Ishizuka T, Ishijima S, Sonoda T, Tatibana M. A novel 39-kDa phosphoribosylpyrophosphate synthetase-associated protein of rat liver. Cloning, high sequence similarity to the catalytic subunits, and a negative regulatory role. *J Biol Chem* 1994;269:8334–8340.
21. Tang W, Li X, Zhu Z, et al. Expression, purification, crystallization and preliminary X-ray diffraction analysis of human phosphoribosyl pyrophosphate synthetase 1 (PRPS1). *Acta Crystallogr Sect F Struct Biol Cryst Commun* 2006;62:432–434.
22. Pui CH, Relling MV, Downing JR. Acute lymphoblastic leukemia. *N Engl J Med* 2004;350:1535–1548.
23. Karran P, Attard N. Thiopurines in current medical practice: molecular mechanisms and contributions to therapy-related cancer. *Nat Rev Cancer* 2008;8:24–36.
24. Zoref E, De Vries A, Sperling O. Mutant feedback-resistant phosphoribosylpyrophosphate synthetase associated with purine overproduction and gout. Phosphoribosylpyrophosphate and purine metabolism in cultured fibroblasts. *J Clin Invest* 1975;56:1093–1099.
25. Christopherson RI, Lyons SD, Wilson PK. Inhibitors of de novo nucleotide biosynthesis as drugs. *Acc Chem Res* 2002;35:961–971.
26. Katashima R, Iwahana H, Fujimura M, et al. Molecular cloning of a human cDNA for the 41-kDa phosphoribosylpyrophosphate synthetase-associated protein. *Biochim Biophys Acta* 1998;1396:245–250.
27. An S, Kumar R, Sheets ED, Benkovic SJ. Reversible compartmentalization of de novo purine biosynthetic complexes in living cells. *Science* 2008;320:103–106.
28. Hanahan D, Weinberg RA. Hallmarks of cancer: the next generation. *Cell* 2011;144:646–674.
29. Becker MA, Heidler SA, Bell GI, et al. Cloning of cDNAs for human phosphoribosylpyrophosphate synthetases 1 and 2 and X chromosome localization of PRPS1 and PRPS2 genes. *Genomics* 1990;8:555–561.
30. de Brouwer AP, van Bokhoven H, Nabuurs SB, Arts WF, Christodoulou J, Duley J. PRPS1 mutations: four distinct syndromes and potential treatment. *Am J Hum Genet* 2010;86:506–518.
31. Eriksen TA, Kadziola A, Bentsen AK, Harlow KW, Larsen S. Structural basis for the function of *Bacillus subtilis* phosphoribosyl-pyrophosphate synthetase. *Nat Struct Biol* 2000;7:303–308.
32. Shalem O, Sanjana NE, Hartenian E, et al. Genome-scale CRISPR-Cas9 knockout screening in human cells. *Science* 2014;343:84–87.
33. Li Y, Feng H, Gu H, et al. The p53-PUMA axis suppresses iPSC generation. *Nat Commun* 2013;4:2174.
34. Lv D, Li Y, Zhang W, et al. TRIM24 is an oncogenic transcriptional co-activator of STAT3 in glioblastoma. *Nat Commun* 2017;8:1454.
35. Gao Y, Yang P, Shen H, et al. Small-molecule inhibitors targeting INK4 protein p18(INK4C) enhance ex vivo expansion of haematopoietic stem cells. *Nat Commun* 2015;6:6328.